Acta Cryst E CRYSTALLOGRAPHIC COMMUNICATIONS

ISSN 2056-9890

Crystal structure and Hirshfeld surface analysis of 2,6-bis[4-(ethoxycarbonyl)-5-methylpyrazol-1-yl]-pyridine

Yevhen Krokhmaliuk,[a] Volodymyr M. Fetyukhin,[b] Yuliya M. Davydenko,[a] Oleksandr S. Vynohradov,[a]* Vadim O. Pavlenko[a] and Mircea-Odin Apostu[c]

[a]Taras Shevchenko National University of Kyiv, Department of Chemistry, 64 str., Volodymyrska, Kyiv 01601, Ukraine, [b]I. F. Lab Ltd., Representative of Life Chemicals Inc., Kyiv, Ukraine, 5 Academician Kukhar St., 02094 Kyiv, Ukraine, and [c]Department of Chemistry, Faculty of Chemistry, Al. I. Cuza University of Iasi, 11 Carol I Blvd, Iasi 700506, Romania. *Correspondence e-mail: oleksandr.vynohradov@knu.ua

Received 29 December 2025
Accepted 18 March 2026

Edited by F. Di Salvo, University of Buenos Aires, Argentina

Keywords: crystal structure; 2,6-bis(pyrazol-1-yl)pyridine derivatives; pyrazolyl; Hirshfeld surface analysis; organic synthesis; hydrogen bonding.

CCDC reference: 2539018

Supporting information: this article has supporting information at journals.iucr.org/e

The title compound (systematic name: ethyl 1-{6-[4-(ethoxycarbonyl)-5-methylpyrazol-1-yl]pyridin-2-yl}-5-methylpyrazole-4-carboxylate), $C_{19}H_{21}N_5O_4$, consists of a central pyridine ring substituted by two functionalized pyrazole rings and crystallizes in the centrosymmetric space group *C*2/*c*. The pyridine–pyrazole and pyrazole–pyrazole dihedral angles are 30.55 (5) and 50.81 (8)°, respectively, indicating significant deviations from coplanarity. An intramolecular C—H···O hydrogen bond stabilizes the molecular conformation. In the crystal, molecules form columns along the *c*-axis, but large centroid separations and offsets between parallel pyridine rings contribute to the absence of π–π stacking. Intermolecular C—H···N and C—H···O hydrogen bonds link molecules into a three-dimensional network. Hirshfeld surface analysis shows that H···H contacts dominate the packing (49.9%), with hydrogen-involving interactions contributing over 90% of all contacts. The molecular shape is moderately anisotropic, with globularity and asphericity values of 0.677 and 0.395, respectively. These results highlight the key role of hydrogen-based interactions in directing the supramolecular organization and crystal cohesion.

1. Chemical context

Complexes based on the ligand 2,6-di(1*H*-pyrazol-1-yl)pyridine attract attention due to their application in coordination chemistry (Halcrow & Kilner, 2003; Jia, 2011). In particular, iron complexes exhibit catalytic activity (Magubane *et al.*, 2016), cross-spin behavior (Pritchard *et al.*, 2009), and manifestations of the Jahn-Teller effect (Kershaw Cook *et al.*, 2015). Iron(II) complexes with diethyl 1,1′-(pyridine-2,6-diyl)*bis*(1*H*-pyrazole-4-carboxylate) demonstrate spin crossover properties that can be induced thermally and by light through the LIESST (light-induced excited spin state trapping) mechanism (García-López *et al.*, 2023). Moreover, the spin state can be reversibly modulated by guest molecules such as $MeNO_2$, MeCN, Me_2CO, and MeCOOH. Considering the coordination versatility and functional potential of pyrazolylpyridine ligands, we aimed to design and synthesize a novel methyl-substituted derivative of 2,6-di(1*H*-pyrazol-1-yl)pyridine and to investigate its structural features using single-crystal X-ray diffraction.

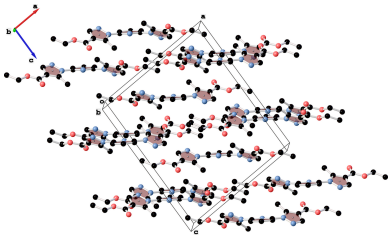

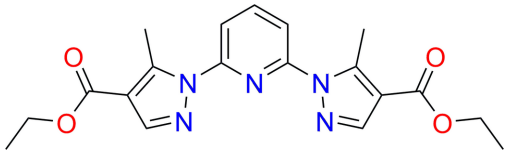

Table 1
Selected geometric parameters (Å, °).

O1—C8	1.3349 (18)	N2—C1	1.4206 (17)
N1—C1	1.3253 (15)	O2—C8	1.2024 (18)
N2—N3	1.3766 (15)		
C1—N1—C1^{i}	116.65 (16)	C2—C1—N2	118.89 (12)
N3—N2—C1	116.58 (11)	O2—C8—O1	123.32 (14)
C5—C4—C7	129.91 (13)	O2—C8—C5	126.21 (14)
N1—C1—N2	116.61 (12)		

Symmetry code: (i) $-x+1, y, -z+\frac{3}{2}$.

2. Structural commentary

In the title compound, $C_{19}H_{21}N_5O_4$, the polycyclic system is composed of three parts: one central pyridine ring substituted by two functionalized pyrazole rings (Fig. 1). The molecule is centrosymmetric with a crystallographic twofold rotation axis (C_2) passing through the N1 and C3 atoms of the central pyridine ring. The dihedral angle between the planes of the pyridine ring and the adjacent pyrazole fragment is 30.55 (5)°, indicating a significant deviation from coplanarity between the two aromatic systems. The dihedral angle between the planes containing two pyrazole rings is 50.81 (8)°. Furthermore, the distance between the centroids of the pyridine ring plane (C1–C3, N1) and one of the pyrazole ring planes (C4–C6, N2, N3) is 3.8535 (7) Å, whereas the centroid-to-centroid distance between the two symmetrically positioned pyrazole moieties is 6.6980 (12) Å. The C8═O2 and C8—O1 bond lengths of 1.2024 (12) and 1.3349 (18) Å, respectively, are in the expected ranges (Cambridge Structural Database; Groom *et al.*, 2016). The molecule is stabilized by an intramolecular C7—H7*B*···O2 hydrogen bond. Selected geometric parameters are given in Table 1.

3. Supramolecular features

In the crystal structure, the molecules are arranged in columns running along the crystallographic *c*-axis (Fig. 2. Despite the parallel orientation of adjacent pyridine ring planes [twist angle = 0.00 (11)°], the centroid-to-centroid distance between them is 8.0879 (2) Å, and the offset is 6.924 (3) Å, which are significantly larger than the values typically associated with effective π–π stacking interactions. These structural parameters clearly indicate the absence of π–π stacking in the crystal. In the crystal, adjacent molecules are linked by C—H···N and C—H···O hydrogen bonds (Table 2).

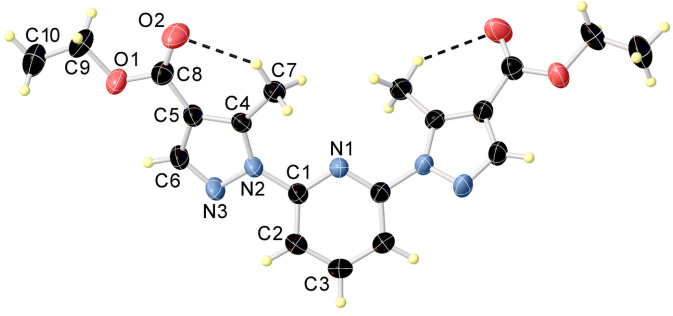

Figure 1
The molecular structure of the title compound, with displacement ellipsoids drawn at the 50% probability level.

Table 2
Hydrogen-bond geometry (Å, °).

D—H···*A*	*D*—H	H···*A*	*D*···*A*	*D*—H···*A*
C7—H7*B*···O2	0.96	2.46 (1)	3.134 (2)	127 (1)
C7—H7*A*···O2	0.96	2.42 (1)	3.290 (2)	151 (1)
C6—H6···N3^{ii}	0.93	2.63 (1)	3.388 (2)	140 (1)

Symmetry code: (ii) $-x+\frac{1}{2}, -y+\frac{1}{2}, -z+1$.

4. Database survey

A search of the Cambridge Structural Database using the WebCSD interface (CSD version 2025.1, May 2025 release; Groom *et al.*, 2016) for the C_5N pyridine ring substituted in the 2- and 6-positions by C_3N_2 pyrazole rings, each bearing a –COO fragment at the 4-position, gave 27 hits. The most closely related structure is UGIPIM (Martinez–Martin *et al.*, 2020), 1,1′-(pyridine-2,6-diyl)bis(1*H*-pyrazole-4-carboxylic acid) acetonitrile solvate. Other similar compounds include coordination complexes of iron with this ligand: XORDEQ, and XORDIU (García-López *et al.*, 2019), as well as a series of iron complexes with diethyl 1,1′-(pyridine-2,6-diyl)bis(1*H*-pyrazole-4-carboxylate) [MIHMID, MIHMUP, MIHNAW, MIHNIE, MIHPAY, MIHPEC, MIHPIG (García-López *et al.*, 2023), TUFXOI (Pritchard *et al.*, 2009)]. The vast majority of the complexes with the above-mentioned ligands are mononuclear species of the general formula MeL_2.

5. Hirshfeld surface analysis

The Hirshfeld surface analysis and the associated two-dimensional fingerprint plots were performed using *Crystal Explorer 21.5* software (Spackman *et al.*, 2021), with a standard resolution of the three-dimensional d_{norm} surfaces plotted over a fixed colour scale of −0.2207 (red) to 1.2076 (blue) a.u. Eight red spots are observed on the d_{norm} surface.

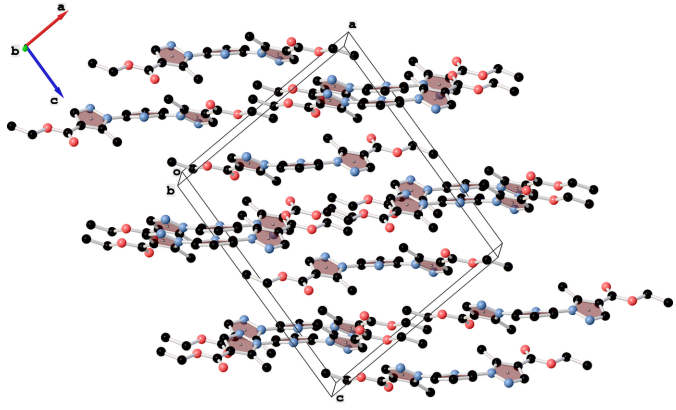

Figure 2
Crystal packing of the title compound viewed along the crystallographic *b* axis. The planes of the pyridine and pyrazole rings are highlighted in red. All hydrogen atoms are omitted for clarity.

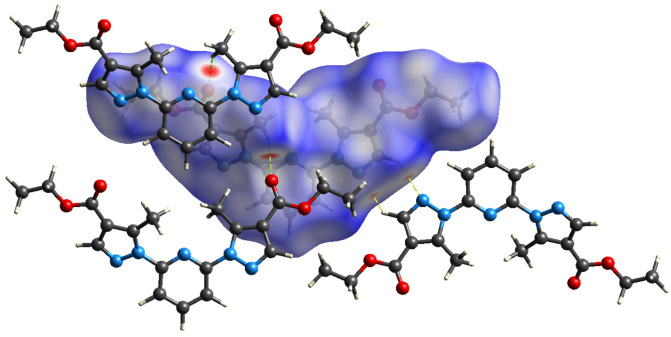

Figure 3
View of the Hirshfeld surface mapped over d_{norm} for the title compound showing C—H···O and C—H···N hydrogen bonds, indicated by green and yellow dashed lines, respectively.

The four dark-red regions correspond to short interatomic contacts and reflect negative d_{norm} values, whereas the remaining four light-red spots indicate weaker intermolecular interactions. The Hirshfeld surfaces mapped over d_{norm} are shown for the H···H, H···C/C···H, H···N/N···H, and H···O/O···H (Figs. 3 and 4), the overall two-dimensional fingerprint plot and the decomposed two-dimensional fingerprint plots are given in Fig. 5. The shortest intermolecular contacts are two pairs of C7–H7*A*···O2 interactions with a length of 2.311 Å, which correspond to contacts between a methyl hydrogen atom of the pyrazole fragment and the carbonyl oxygen atom of the ester (COOEt) group of a neighboring molecule. Considering the weak and predominantly electrostatic character of the intermolecular C—H···O hydrogen bonds, their contribution to the stabilization of the crystal packing is minor. Additionally, two pairs of C6—H6···N3 contacts measuring 2.512 Å are observed, representing interactions between the hydrogen and nitrogen atoms of pyrazole fragments from adjacent molecules. H···H contacts make 49.9% contribution, which is mostly associated with terminal positions of H atoms and is chemically insignificant. The most significant meaningful interactions to the overall crystal packing are from H···C/C···H (15.8%),

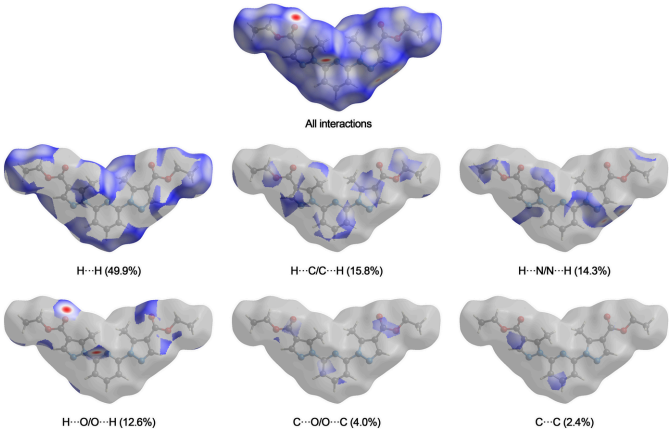

Figure 4
Hirshfeld surface representations with the function d_{norm} plotted onto the surface for individual interactions.

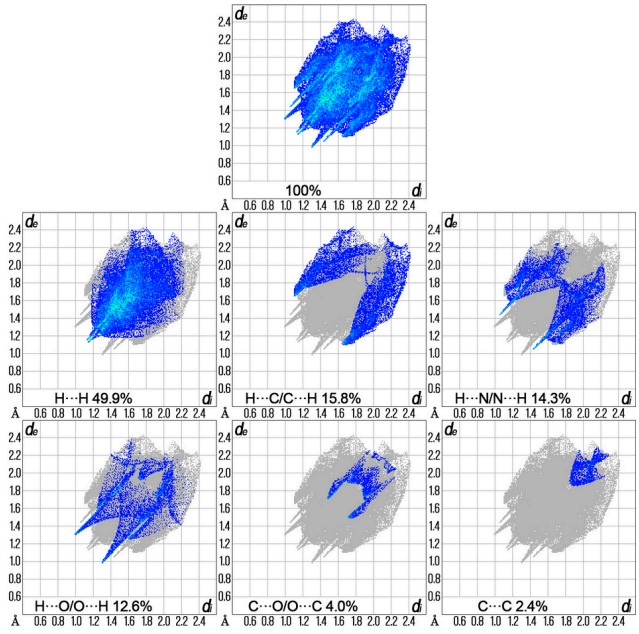

Figure 5
The overall two-dimensional fingerprint plot and those delineated into specified interactions.

H···N/N···H (14.3%), and H···O/O···H (12.6%) contacts. There is a small contribution from C···O/O···C (4.0%) and C···C (2.4%), O···O (0.4%) and O···N/N···O (0.5%) weak intermolecular contacts. The relative percentage contributions to the overall Hirshfeld surface by elements: H···all atoms – 68.7%, C···all atoms – 13.3%, O···all atoms – 9.6% and N···all atoms – 8.4%. The data clearly highlight the dominant role of hydrogen-involving interactions in the formation and stabilization of the crystal packing. The overwhelming contribution from H···H and other hydrogen-related contacts accounts for over 90% of all intermolecular interactions. These findings indicate that hydrogen-based interactions are the principal driving force behind the supramolecular organization and efficient molecular packing within the crystal lattice. The calculated quantitative physical properties of the Hirshfeld surface — molecular volume (470.13 Å^3), surface area (431.66 Å^2), globularity (0.677), and asphericity (0.395) — provide insights into the molecular shape and packing characteristics. The moderate asphericity value indicates a noticeable deviation from spherical symmetry, suggesting that the molecular shape is somewhat elongated or irregular. In addition, the globularity value significantly below 1 implies that the molecular surface is less compact and more complex than a perfect sphere. These parameters suggest an anisotropic and non-spherical molecular shape, which correspondingly influences the packing of molecules in the crystal.

6. Synthesis and crystallization

Ethyl 3-oxobutanoate (2.06 g, 15.8 mmol) and 1,1-dimethoxy-*N*,*N*-dimethylmethanamine (2.56 g, 17.4 mmol) were placed in

Table 3
Experimental details.

Crystal data	
Chemical formula	$C_{19}H_{21}N_5O_4$
M_r	383.41
Crystal system, space group	Monoclinic, *C*2/*c*
Temperature (K)	293
a, *b*, *c* (Å)	13.8701 (5), 8.3233 (3), 16.6408 (6)
β (°)	94.279 (3)
V (Å^3)	1915.76 (12)
Z	4
Radiation type	Mo $K\alpha$
μ (mm^{-1})	0.10
Crystal size (mm)	0.3 × 0.2 × 0.2
Data collection	
Diffractometer	Xcalibur, Eos
Absorption correction	Multi-scan (*CrysAlis PRO*; Rigaku OD, 2025)
T_{min}, T_{max}	0.988, 1.000
No. of measured, independent and observed [$I > 2\sigma(I)$] reflections	6654, 2258, 1846
R_{int}	0.017
(sin $\theta/\lambda)_{max}$ (Å^{-1})	0.689
Refinement	
$R[F^2 > 2\sigma(F^2)]$, $wR(F^2)$, S	0.047, 0.121, 1.06
No. of reflections	2258
No. of parameters	131
H-atom treatment	H-atom parameters constrained
$\Delta\rho_{max}$, $\Delta\rho_{min}$ (e Å^{-3})	0.21, −0.15

Computer programs: *CrysAlis PRO* (Rigaku OD, 2025), *SHELXT* (Sheldrick, 2015*a*), *SHELXL2019/3* (Sheldrick, 2015*b*) and *OLEX2* (Dolomanov *et al.*, 2009).

a round-bottom flask and refluxed for 2 h. After cooling to room temperature, acetic acid (28 mL) and freshly prepared 2,6-dihydrazinylpyridine (Brien *et al.*, 2006) (1.00 g, 7.2 mmol) were added, and the solution was refluxed overnight. The reaction mixture was evaporated under reduced pressure, and the residue was dissolved in dichloromethane. The organic layer was extracted twice with a saturated aqueous solution of $NaHCO_3$. The organic phase was dried over Na_2SO_4 and evaporated under reduced pressure. The crude product was purified by flash chromatography using a gradient of EtOAc/Hex (10:1 to 1:1, *v*/*v*). As a result, diethyl 1,1′-(pyridine-2,6-diyl)bis(5-methyl-1*H*-pyrazole-4-carboxylate) was obtained as a yellow powder (2.4 g, 87%). ^{1}H NMR (400 MHz, chloroform-*d*) δ 8.13–7.99 (*m*, 3H, Ar-H), 7.85 (*d*, J = 8.1 Hz, 2H, Ar-H), 4.34 (*q*, J = 7.1 Hz, 4H, CH_2), 2.90 (*s*, 6H, CH_3), 1.38 (*t*, J = 7.1 Hz, 6H, CH_3); ^{13}C NMR (101 MHz, chloroform-*d*) δ 163.62, 150.97, 145.14, 142.86, 141.31, 116.62, 114.59, 60.29, 14.51, 13.17; m. p. 427 K;

Clear, pale-yellow prismatic crystals suitable for X-ray diffraction were obtained from an Et_2O/CH_2Cl_2 solution by evaporation in the open air.

7. Refinement

Crystal data, data collection and structure refinement details are summarized in Table 3. All hydrogen atoms were positioned geometrically and refined isotropically using a riding model with C—H = 0.96 Å for CH_3 groups, 0.97 Å for CH_2 groups, and 0.93 Å for CH groups. The isotropic displacement parameters were set at U_{iso}(H) = 1.5 U_{eq}(C) for methyl hydrogens and U_{iso}(H) = 1.2 U_{eq}(C) for all other hydrogen atoms.

Acknowledgements

Vadym Pavlenko is grateful to the II European Chemistry School for Ukrainians for providing a comprehensive overview of current trends in European chemical science (https://acmin.agh.edu.pl/en/detail/s/ii-european-chemistry-school-for-ukrainians). The authors also are grateful to the FAIRE programme provided by the Cambridge Crystallographic Data Centre (CCDC) for the opportunity to use the Cambridge Structural Database (CSD) and associated software.

Funding information

Funding for this research was provided by: The Ministry of Education and Science of Ukraine through grant No. 24DF037-04N (RN/61-2024).

References

Brien, K. A., Garner, C. M. & Pinney, K. G. (2006). *Tetrahedron* **62**, 3663–3666.
Dolomanov, O. V., Bourhis, L. J., Gildea, R. J., Howard, J. A. K. & Puschmann, H. (2009). *J. Appl. Cryst.* **42**, 339–341.
García-López, V., El Jastimi, H. E. M., Juráková, J., Clemente-León, M. & Coronado, E. (2023). *Cryst. Growth Des.* **23**, 2730–2738.
García-López, V., Palacios-Corella, M., Cardona-Serra, S., Clemente-León, M. & Coronado, E. (2019). *Chem. Commun.* **55**, 12227–12230.
Groom, C. R., Bruno, I. J., Lightfoot, M. P. & Ward, S. C. (2016). *Acta Cryst.* B**72**, 171–179.
Halcrow, M. A. & Kilner, C. A. (2003). *Acta Cryst.* C**59**, m61–m63.
Jia, C.-X. (2011). *Acta Cryst.* E**67**, m1059.
Kershaw Cook, L. J., Thorp-Greenwood, F. L., Comyn, T. P., Cespedes, O., Chastanet, G. & Halcrow, M. A. (2015). *Inorg. Chem.* **54**, 6319–6330.
Magubane, M. N., Nyamato, G. S., Ojwach, S. O. & Munro, O. Q. (2016). *RSC Adv.* **6**, 65205–65221.
Martinez-Martin, P., Perles, J. & Rodriguez-Ubis, J. C. (2020). *Crystals* **10**, 69.
Pritchard, R., Kilner, C. A., Barrett, S. A. & Halcrow, M. A. (2009). *Inorg. Chim. Acta* **362**, 4365–4371.
Rigaku OD (2025). *CrysAlis PRO*. Rigaku Oxford Diffraction, Yarnton, England.
Sheldrick, G. M. (2015*a*). *Acta Cryst.* A**71**, 3–8.
Sheldrick, G. M. (2015*b*). *Acta Cryst.* C**71**, 3–8.
Spackman, P. R., Turner, M. J., McKinnon, J. J., Wolff, S. K., Grimwood, D. J., Jayatilaka, D. & Spackman, M. A. (2021). *J. Appl. Cryst.* **54**, 1006–1011.

supporting information

Acta Cryst. (2026). E**82**, 404-407 [https://doi.org/10.1107/S2056989026002860]

Crystal structure and Hirshfeld surface analysis of 2,6-bis[4-(ethoxycarbonyl)-5-methylpyrazol-1-yl]pyridine

Yevhen Krokhmaliuk, Volodymyr M. Fetyukhin, Yuliya M. Davydenko, Oleksandr S. Vynohradov, Vadim O. Pavlenko and Mircea-Odin Apostu

Computing details

Ethyl 1-{6-[4-(ethoxycarbonyl)-5-methylpyrazol-1-yl]\ pyridin-2-yl}-5-methylpyrazole-4-carboxylate

Crystal data

$C_{19}H_{21}N_5O_4$
$M_r = 383.41$
Monoclinic, $C2/c$
$a = 13.8701$ (5) Å
$b = 8.3233$ (3) Å
$c = 16.6408$ (6) Å
$\beta = 94.279$ (3)°
$V = 1915.76$ (12) Å^3
$Z = 4$
$F(000) = 808$
$D_x = 1.329$ Mg m^{-3}
Mo $K\alpha$ radiation, $\lambda = 0.71073$ Å
Cell parameters from 3164 reflections
$\theta = 2.5$–$28.2°$
$\mu = 0.10$ mm^{-1}
$T = 293$ K
Prism, clear light colourless
0.3 × 0.2 × 0.2 mm

Data collection

Xcalibur, Eos diffractometer
Radiation source: fine-focus sealed X-ray tube, Enhance (Mo) X-ray Source
Graphite monochromator
Detector resolution: 16.1593 pixels mm^{-1}
ω scans
Absorption correction: multi-scan (CrysAlisPro; Rigaku OD, 2025)
$T_{min} = 0.988$, $T_{max} = 1.000$
6654 measured reflections
2258 independent reflections
1846 reflections with $I > 2\sigma(I)$
$R_{int} = 0.017$
$\theta_{max} = 29.3°$, $\theta_{min} = 2.5°$
$h = -17\rightarrow19$
$k = -10\rightarrow9$
$l = -21\rightarrow22$

Refinement

Refinement on F^2
Least-squares matrix: full
$R[F^2 > 2\sigma(F^2)] = 0.047$
$wR(F^2) = 0.121$
$S = 1.06$
2258 reflections
131 parameters
0 restraints
Primary atom site location: dual
Hydrogen site location: inferred from neighbouring sites
H-atom parameters constrained
$w = 1/[\sigma^2(F_o^2) + (0.0553P)^2 + 0.863P]$ where $P = (F_o^2 + 2F_c^2)/3$
$(\Delta/\sigma)_{max} < 0.001$
$\Delta\rho_{max} = 0.21$ e Å^{-3}
$\Delta\rho_{min} = -0.15$ e Å^{-3}
Extinction correction: SHELXL-2019/2 (Sheldrick 2015b), $Fc^* = kFc[1+0.001xFc^2\lambda^3/\sin(2\theta)]^{-1/4}$
Extinction coefficient: 0.0103 (11)

Special details

Geometry. All esds (except the esd in the dihedral angle between two l.s. planes) are estimated using the full covariance matrix. The cell esds are taken into account individually in the estimation of esds in distances, angles and torsion angles; correlations between esds in cell parameters are only used when they are defined by crystal symmetry. An approximate (isotropic) treatment of cell esds is used for estimating esds involving l.s. planes.

Fractional atomic coordinates and isotropic or equivalent isotropic displacement parameters (Å²)

	x	*y*	*z*	U_{iso}*/U_{eq}
O1	0.12747 (8)	0.67265 (14)	0.53552 (7)	0.0531 (3)
N1	0.500000	0.37887 (19)	0.750000	0.0334 (4)
N2	0.35918 (8)	0.38495 (14)	0.66370 (7)	0.0362 (3)
O2	0.19474 (10)	0.82118 (15)	0.63654 (8)	0.0689 (4)
N3	0.31854 (9)	0.31425 (15)	0.59446 (8)	0.0455 (3)
C4	0.32038 (9)	0.53186 (16)	0.67745 (8)	0.0336 (3)
C5	0.25205 (10)	0.55721 (17)	0.61385 (8)	0.0375 (3)
C1	0.43158 (9)	0.29526 (17)	0.70887 (8)	0.0356 (3)
C6	0.25485 (11)	0.41904 (19)	0.56543 (9)	0.0450 (4)
H6	0.215840	0.403902	0.518117	0.054*
C7	0.34643 (11)	0.63313 (18)	0.74956 (9)	0.0428 (4)
H7A	0.339730	0.571246	0.797503	0.064*
H7B	0.304232	0.724593	0.749239	0.064*
H7C	0.412121	0.668872	0.748431	0.064*
C8	0.19070 (11)	0.69797 (18)	0.59872 (9)	0.0422 (4)
C2	0.42718 (12)	0.12910 (19)	0.70670 (10)	0.0507 (4)
H2	0.377389	0.075376	0.677365	0.061*
C3	0.500000	0.0471 (3)	0.750000	0.0602 (7)
H3	0.500001	−0.064607	0.749999	0.072*
C9	0.05946 (13)	0.7998 (2)	0.51338 (10)	0.0561 (5)
H9A	0.093542	0.898624	0.503183	0.067*
H9B	0.017386	0.818789	0.556416	0.067*
C10	0.00211 (15)	0.7460 (3)	0.43922 (12)	0.0757 (6)
H10A	0.044512	0.728822	0.396993	0.113*
H10B	−0.044625	0.826846	0.422786	0.113*
H10C	−0.030589	0.647511	0.449980	0.113*

Atomic displacement parameters (Å²)

	U^{11}	U^{22}	U^{33}	U^{12}	U^{13}	U^{23}
O1	0.0482 (6)	0.0533 (7)	0.0554 (7)	0.0152 (5)	−0.0126 (5)	−0.0053 (5)
N1	0.0312 (8)	0.0322 (8)	0.0365 (8)	0.000	−0.0007 (6)	0.000
N2	0.0338 (6)	0.0347 (6)	0.0389 (6)	0.0012 (5)	−0.0048 (5)	−0.0082 (5)
O2	0.0894 (10)	0.0520 (8)	0.0620 (8)	0.0260 (7)	−0.0153 (7)	−0.0174 (6)
N3	0.0445 (7)	0.0438 (7)	0.0459 (7)	0.0054 (6)	−0.0125 (6)	−0.0168 (5)
C4	0.0322 (7)	0.0317 (7)	0.0369 (7)	−0.0019 (5)	0.0018 (5)	−0.0033 (5)
C5	0.0341 (7)	0.0392 (8)	0.0385 (7)	0.0012 (6)	−0.0011 (5)	−0.0060 (6)
C1	0.0342 (7)	0.0348 (7)	0.0372 (7)	0.0003 (5)	−0.0003 (6)	−0.0032 (5)
C6	0.0399 (8)	0.0477 (9)	0.0453 (8)	0.0045 (6)	−0.0110 (6)	−0.0129 (7)

C7	0.0487 (8)	0.0381 (8)	0.0405 (8)	0.0033 (6)	−0.0042 (6)	−0.0079 (6)
C8	0.0425 (8)	0.0454 (9)	0.0386 (7)	0.0067 (6)	0.0023 (6)	−0.0028 (6)
C2	0.0522 (9)	0.0356 (8)	0.0615 (10)	−0.0038 (7)	−0.0137 (8)	−0.0054 (7)
C3	0.0675 (16)	0.0306 (12)	0.0790 (17)	0.000	−0.0187 (13)	0.000
C9	0.0505 (9)	0.0638 (11)	0.0537 (9)	0.0222 (8)	0.0017 (8)	0.0101 (8)
C10	0.0643 (12)	0.0864 (15)	0.0725 (13)	0.0117 (11)	−0.0204 (10)	0.0125 (11)

Geometric parameters (Å, º)

O1—C8	1.3349 (18)	C6—H6	0.9300
O1—C9	1.4469 (19)	C7—H7A	0.9600
N1—C1^{i}	1.3253 (15)	C7—H7B	0.9600
N1—C1	1.3253 (15)	C7—H7C	0.9600
N2—N3	1.3766 (15)	C2—H2	0.9300
N2—C4	1.3622 (17)	C2—C3	1.3770 (19)
N2—C1	1.4206 (17)	C3—H3	0.9300
O2—C8	1.2024 (18)	C9—H9A	0.9700
N3—C6	1.3080 (19)	C9—H9B	0.9700
C4—C5	1.3832 (18)	C9—C10	1.487 (3)
C4—C7	1.4886 (18)	C10—H10A	0.9600
C5—C6	1.406 (2)	C10—H10B	0.9600
C5—C8	1.459 (2)	C10—H10C	0.9600
C1—C2	1.385 (2)		
C8—O1—C9	117.56 (13)	H7B—C7—H7C	109.5
C1—N1—C1^{i}	116.65 (16)	O1—C8—C5	110.47 (12)
N3—N2—C1	116.58 (11)	O2—C8—O1	123.32 (14)
C4—N2—N3	112.47 (11)	O2—C8—C5	126.21 (14)
C4—N2—C1	130.95 (11)	C1—C2—H2	121.6
C6—N3—N2	104.31 (11)	C3—C2—C1	116.88 (15)
N2—C4—C5	105.37 (11)	C3—C2—H2	121.6
N2—C4—C7	124.65 (12)	C2—C3—C2^{i}	120.6 (2)
C5—C4—C7	129.91 (13)	C2—C3—H3	119.7
C4—C5—C6	105.49 (12)	C2^{i}—C3—H3	119.7
C4—C5—C8	127.74 (13)	O1—C9—H9A	110.4
C6—C5—C8	126.76 (13)	O1—C9—H9B	110.4
N1—C1—N2	116.61 (12)	O1—C9—C10	106.82 (16)
N1—C1—C2	124.50 (13)	H9A—C9—H9B	108.6
C2—C1—N2	118.89 (12)	C10—C9—H9A	110.4
N3—C6—C5	112.36 (12)	C10—C9—H9B	110.4
N3—C6—H6	123.8	C9—C10—H10A	109.5
C5—C6—H6	123.8	C9—C10—H10B	109.5
C4—C7—H7A	109.5	C9—C10—H10C	109.5
C4—C7—H7B	109.5	H10A—C10—H10B	109.5
C4—C7—H7C	109.5	H10A—C10—H10C	109.5
H7A—C7—H7B	109.5	H10B—C10—H10C	109.5
H7A—C7—H7C	109.5		

N1—C1—C2—C3	−0.6 (2)	C1^{i}—N1—C1—N2	−178.96 (14)
N2—N3—C6—C5	−0.20 (18)	C1^{i}—N1—C1—C2	0.32 (12)
N2—C4—C5—C6	0.23 (15)	C1—N2—N3—C6	179.43 (12)
N2—C4—C5—C8	−178.84 (14)	C1—N2—C4—C5	−179.27 (13)
N2—C1—C2—C3	178.64 (11)	C1—N2—C4—C7	−2.0 (2)
N3—N2—C4—C5	−0.37 (16)	C1—C2—C3—C2^{i}	0.29 (10)
N3—N2—C4—C7	176.90 (13)	C6—C5—C8—O1	6.9 (2)
N3—N2—C1—N1	149.52 (12)	C6—C5—C8—O2	−172.99 (17)
N3—N2—C1—C2	−29.80 (19)	C7—C4—C5—C6	−176.84 (15)
C4—N2—N3—C6	0.36 (17)	C7—C4—C5—C8	4.1 (3)
C4—N2—C1—N1	−31.6 (2)	C8—O1—C9—C10	176.62 (15)
C4—N2—C1—C2	149.05 (16)	C8—C5—C6—N3	179.07 (14)
C4—C5—C6—N3	−0.02 (18)	C9—O1—C8—O2	−1.4 (2)
C4—C5—C8—O1	−174.22 (14)	C9—O1—C8—C5	178.68 (13)
C4—C5—C8—O2	5.9 (3)		

Symmetry code: (i) −*x*+1, *y*, −*z*+3/2.

Hydrogen-bond geometry (Å, º)

D—H···*A*	*D*—H	H···*A*	*D*···*A*	*D*—H···*A*
C7—H7*B*···O2	0.96	2.46 (1)	3.134 (2)	127 (1)
C7—H7*A*···O2	0.96	2.42 (1)	3.290 (2)	151 (1)
C6—H6···N3^{ii}	0.93	2.63 (1)	3.388 (2)	140 (1)

Symmetry code: (ii) −*x*+1/2, −*y*+1/2, −*z*+1.